ACS OMEGA

http://pubs.acs.org/journal/acsodf

Article

Comparative Study of Sorbents for Spray Dry Scrubbing of SO_2 from Flue Gases

Lawrence Koech,* Raymond C. Everson, Burgert Hattingh, Hilary Rutto, Letsabisa Lerotholi, and Hein WJP Neomagus

Cite This: *ACS Omega* 2023, 8, 23401−23411

Read Online

ACCESS | Metrics & More | Article Recommendations

ABSTRACT: This study presents the findings of an investigation involving the absorption of SO_2 from flue gases, using three different sorbents, in a spray dryer. Experimentation involved the evaluation of three sorbents, i.e., hydrated lime ($Ca[OH]_2$), limestone ($CaCO_3$), and trona ($Na_2CO_3{\cdot}NaHCO_3{\cdot}2H_2O$), and their relevant properties, for flue gas desulfurization by spray dry scrubbing. Experiments were conducted to explore the effects of spray characteristics in the spray drying scrubber on SO_2 removal efficiency using the selected sorbents. The ranges of various operating parameters were considered, including the stoichiometric molar ratio of (1.0−2.5), the inlet gas phase temperature of (120−180 °C), and an inlet SO_2 concentration of 1000 ppm. The use of trona gave better SO_2 removal characteristics; a high SO_2 removal efficiency of 94% was recorded at an inlet gas phase temperature of 120 °C and a stoichiometric molar ratio of 1.5. Under the same operating conditions, $Ca[OH]_2$ and $CaCO_3$ gave 82 and 76% SO_2 removal efficiency, respectively. Analysis of the desulfurization products by X-ray fluorescence (XRF) and Fourier transform infrared (FTIR) spectroscopy revealed the presence of $CaSO_3/Na_2SO_3$, a product of the semidry desulfurization reaction. A significant proportion of unreacted sorbent was observed when $Ca[OH]_2$ and $CaCO_3$ sorbents were used at a stoichiometric ratio of 2.0. Trona also gave the highest degree of conversion (96%) at a stoichiometric molar ratio of 1.0. $Ca[OH]_2$ and $CaCO_3$ gave 63 and 59%, respectively, under the same operating conditions.

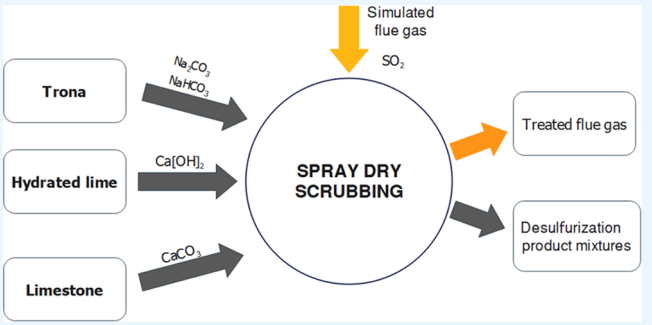

1. INTRODUCTION

Flue gas desulfurization (FGD) is a commercially proven technology for the removal of SO_2 from industrial flue gas streams. There are presently three types of FGD technology for the removal of SO_2: dry, semidry, and wet FGD technology. The wet limestone FGD process accounts for the largest market share of the FGD systems currently used in large utility boilers.[1] It has been a preferred choice for many utility plants due to its reliability, high SO_2 removal efficiency, and the availability of the sorbent (limestone, $CaCO_3$). On the other hand, interest in the spray drying FGD technology has increased over the past decade,[2] for various reasons, e.g., (a) reduced installation and operating costs, (b) ease of retrofit to existing plants due to reduced footprint requirement, (c) ease of product handling with no requirement for sludge handling equipment and the associated maintenance, and (d) reduced water usage.[3−5] Despite the high reagent costs and low degree of utilization in spray drying scrubber process (typically 40−70%), it has been proven to have the ability to remove SO_2 from flue gas well below legislative limits.[6,7]

In the spray drying scrubber process, a concentrated sorbent slurry is introduced at the top of the scrubber via a two-fluid nozzle or rotary atomizers, producing a fine mist of droplets containing the sorbent, which then reacts with SO_2 contained in the untreated flue gas from a coal-fired boiler.[8] The water in the slurry humidifies and allows cooling of the flue gas from higher temperatures to about 17 °C above the water saturation temperature.[9] This process, therefore, requires careful control of the amount of water fed into the spray dryer to avoid complete saturation of the flue gas.[1] The residence time in the absorption chamber should be sufficient to allow SO_2 and other gases such as SO_3 and HCl to react with the sorbent.[10] In the spray chamber, evaporation of water and drying of the droplets takes place as it flows downward, with concurrent formation of a dry waste product containing mostly sulfites, unreacted hydrated lime ($Ca[OH]_2$), and traces of sulfate salts.[10,11] Part of the dry waste is collected at the bottom of the

Received: January 5, 2023
Accepted: May 29, 2023
Published: June 23, 2023

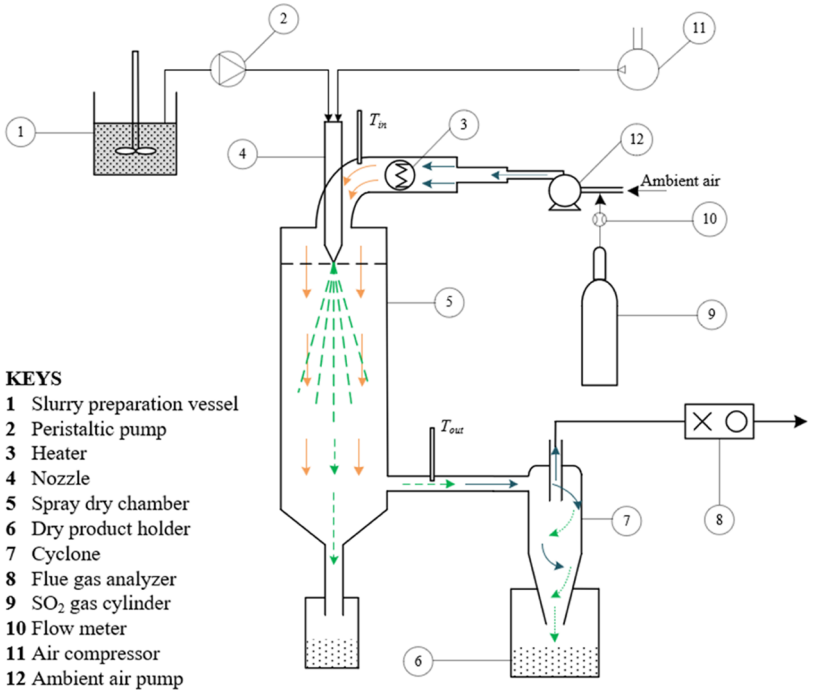

Figure 1. Experimental setup used for spray dry scrubbing of SO_2 (adapted in part with permission from B-290 Spray Dryer operation manual.[19] Copyright 2018 Buchi).

scrubber, while the remaining suspended solids are removed by a particulate control device such as a baghouse or an electrostatic precipitator (ESP).[12]

The operating cost of the FGD process mainly depends on the following factors: the amount and type of sorbent used, utility (water and electricity) consumption, maintenance required, and the end-product disposal cost.[7] Sorbent performance in spray dry scrubbing of SO_2 is influenced by several factors: e.g., gas humidity, liquid-to-gas ratio, stoichiometric molar ratio, flue gas concentration, and approach to saturation temperature, among others.[10] Over time, remarkable strides have been made to improve the efficiency of this process.[13]

The spray drying scrubber process utilizes various sorbents for the absorption of SO_2 from flue gas, typically appropriate alkali sorbents, either calcium- or sodium-based. The most commonly used sorbents include hydrated lime, precalcined limestone, and sodium carbonate; sorbents are typically prepared by continuously mixing in a slurry tank to avoid sedimentation and agglomeration.[14] Although hydrated lime is expensive compared to limestone, it has been extensively used in spray drying scrubber FGD processes due to its high reactivity toward SO_2. Despite the capabilities exhibited by existing spray drying scrubbers employing hydrated lime as a sorbent, poor sorbent utilization remains a challenge. Trona is a naturally occurring mineral, with abundant worldwide deposits; it is mainly composed of Na_2CO_3 and $NaHCO_3$.[15] It is highly alkaline and soluble in water, making it a useful reagent for the scrubbing of SO_2. It has been tested and proven to be highly reactive toward SO_2, with greater conversion levels approaching unity.[16,17] Trona now offers the possibility of using alternative sorbents in the spray drying scrubber process, for enhanced performance, against the well-established wet FGD technology. Sodium-based sorbents such as trona have mostly been tested for dry sorbent injection processes with limited attention dedicated to their application in spray drying FGD.[15,18]

The comparison of sorbents in spray dry scrubbing of SO_2 is of utmost importance as it determines the most effective method of removing sulfur dioxide from flue gas streams generated by power plants and industrial facilities. The comparison assesses the absorption and retention abilities of each sorbent, as well as its efficiency in the spray drying process. By determining which sorbent is the most suitable for a particular application, informed decisions can be made on which one to use, taking into consideration factors such as cost, availability, and sustainability. The outcome of this comparison plays a vital role in reducing sulfur dioxide emissions, thus contributing to the attainment of environmental protection goals. A thorough review of the literature by the authors provided limited to no published research on the performance comparison of hydrated lime, limestone, and trona for spray dry scrubbing of SO_2.

This paper aims to investigate the performance characteristics of suitable sorbents for spray dry scrubbing of SO_2 from flue gases, using a laboratory-scale spray dryer. Of particular interest is utilizing locally available sorbents suitable for semidry FGD applications, with respect to South African coal-fired power stations located in semiarid water-scarce regions. Appropriate sorbents (hydrated lime, limestone, and trona) for the spray dry scrubbing FGD process were identified, characterized, and then subjected to various experimental conditions to compare their performances in terms of SO_2 scrubbing in a spray dryer. The spray drying characteristics such as inlet gas phase temperature, stoichiometric molar ratio (SR), slurry concentration, and flow rate were closely monitored while controlling the input and output state variables.

2. EXPERIMENTAL SECTION

Experiments were carried out using a co-current flow laboratory-scale Buchi B290 mini spray dryer. Figure 1 shows a schematic of the spray drying setup comprising a

https://doi.org/10.1021/acsomega.3c00064
ACS Omega 2023, 8, 23401−23411

Table 1. Sorbents: Chemical Analysis (Major Components, Determined by XRF)

	components (wt %)						
	Na_2O	MgO	Al_2O_3	SiO_2	MgO	CaO	LOI
hydrated lime ($Ca[OH]_2$)	0.15	0.73	0.51	4.82	0.73	58.47	34.88
limestone ($CaCO_3$)	0.00	0.58	0.23	0.79	1.17	54.43	42.54
trona ($Na_2CO_3{\cdot}NaHCO_3{\cdot}2H_2O$)	51.58	0.00	0.00	0.00	0.00	0.07	48.33

Table 2. Chemical Composition of the Sorbents Determined by XRD Analysis

	portlandite ($Ca[OH]_2$)	calcite ($CaCO_3$)	quartz (SiO_2)	nahcolite ($NaHCO_3$)	dolomite ($CaMg[CO_3]_2$)	kaolinite ($Al_2Si_2O_5[OH]_4$)
hydrated lime	86.9	12.2	0.9	0.0	0.0	0.0
limestone	0.0	95.3	0.9	0.0	3.7	0.1
trona	0.0	0.0	0.0	100.0	0.0	0.0

slurry preparation tank, spray drying chamber, flue gas analyzer, and other accessories. The spray chamber is made of cylindrical borosilicate glass 3.3 with a diameter of 0.16 m and a height of 0.6 m.

Three different sorbents were identified and investigated: commercial-grade hydrated lime supplied by Kayla Africa, South Africa (86.9 wt % $Ca[OH]_2$), limestone supplied by PPC Northern Cape, South Africa (95.3 wt % $CaCO_3$), and commercial-grade trona supplied by Kayla Africa, South Africa (100.0 wt % $NaHCO_3$). Their chemical properties are summarized in Table 1, as determined by X-ray fluorescence (XRF), and Table 2, as determined by X-ray diffraction (XRD).

The sorbent slurries were prepared by continuously mixing the sorbent with an appropriate volume of water in a reaction vessel to obtain the desired solids concentration of 6−12 wt %. These limits were based on the results of trial experiments and considering industrial flue gas treatment conditions. The prepared sorbent slurry was then introduced via a two-fluid nozzle (nozzle cap, 1.4 mm; nozzle tip, 0.7 mm) into the spray dryer at a controlled mass flow rate to maintain the required stoichiometric molar ratios.

The simulated flue gas was generated by blending 99 vol % SO_2 with ambient air at controlled flow to achieve the required inlet SO_2 concentration. The temperature of the inlet flue gas was regulated using an electrical heater located at the spray chamber entry. The two-fluid nozzle in the spray chamber disperses the sorbent slurry to produce fine droplets, which come into contact with the heated flue gas. In the spray chamber, simultaneous drying, evaporation, and absorption occur,[3] resulting in a final dry product that is collected at the bottom of the chamber and captured by the cyclone separator. Throughout each experimental run, the flue gas flowed continuously, and the sorbent slurry was sprayed continuously. Flue gas was continuously sampled at five points (95 mm apart) along the chamber (see Figure 1) to analyze SO_2 concentrations (ppm). The ranges of the operating parameters are presented in Table 3. The stoichiometric molar ratios of the three sorbents, ranging from 1 to 2.5 (based on prescribed ranges published in other works),[20−23] was controlled by varying the feed slurry concentration (6−12%) while keeping a constant gas phase SO_2 concentration of 1000 ppm and inlet gas phase temperature of 140 °C, typical of industrial untreated flue gas streams.

Various analytical techniques were used to determine the physiochemical properties of the sorbents and the dry desulfurization products. The chemical composition of the samples (expressed as oxides of the particular elemental species) was determined using XRF analysis. X-ray diffraction (XRD), using a Malvern Panalytical Aeris diffractometer with a PIXcel detector and fixed slits with Fe-filtered Co-Kα radiation, was used for qualitative analysis of the samples. The phases present were identified using X'Pert HighScore Plus software. The functional groups present in the samples were determined by Fourier transform infrared (FTIR) analysis using the PerkinElmer Spectrum Two instrument, which enabled the observation of a variety of functional groups on the desulfurization products. The morphological structures of the samples and the structural changes of the different sorbents after desulfurization were determined using a Philips XL-30S scanning electron microscopy (SEM) machine. Malvern Mastersizer 2000 machine was used to determine sorbent particle size measurements in the range of 0.01−2000 μm.

Table 3. Desulfurization: Process Parameters and Equipment Specifications

equipment specification (unit)	range
feed air flow rate (m^3/h)	20−35
atomizing air flow rate (m^3/h)	0.35−0.75
maximum air inlet temperature (°C)	220
maximum slurry feed rate (kg/h)	2.0
process parameter (unit)	**range**
inlet gas phase temperature (°C)	120−180
slurry solid concentration (wt %)	6−12
stoichiometric molar ratio (Ca/S, Na/S) (mol/mol)	1−2.5
slurry feed rate (kg/h)	0.8
inlet flue gas SO_2 concentration (ppm)	1000

3. RESULTS AND DISCUSSION

3.1. Analysis of Sorbent Properties. The sorbents were characterized by X-ray fluorescence (XRF) and X-ray diffraction (XRD) analyses. Table 1 presents the results of the XRF analysis, which determined the elemental composition of the sorbents' minerals. Figure 2 shows the XRD diffraction patterns of the sorbents. Based on the XRF results in Table 1, it was found that each sorbent comprised various components. Hydrated lime and limestone were identified as having calcium as the dominant component, represented by CaO in the XRF analysis. The presence of Ca is clearly discernible in the XRD analysis (Table 2), indicating that calcite ($CaCO_3$) is a major crystalline component of the limestone sorbent. The relative phase amount of calcite was found to be 95.3 wt %, according to Table 2. Portlandite ($Ca[OH]_2$) was found to be the dominant component in hydrated lime, with a relative phase

https://doi.org/10.1021/acsomega.3c00064
ACS Omega 2023, 8, 23401−23411

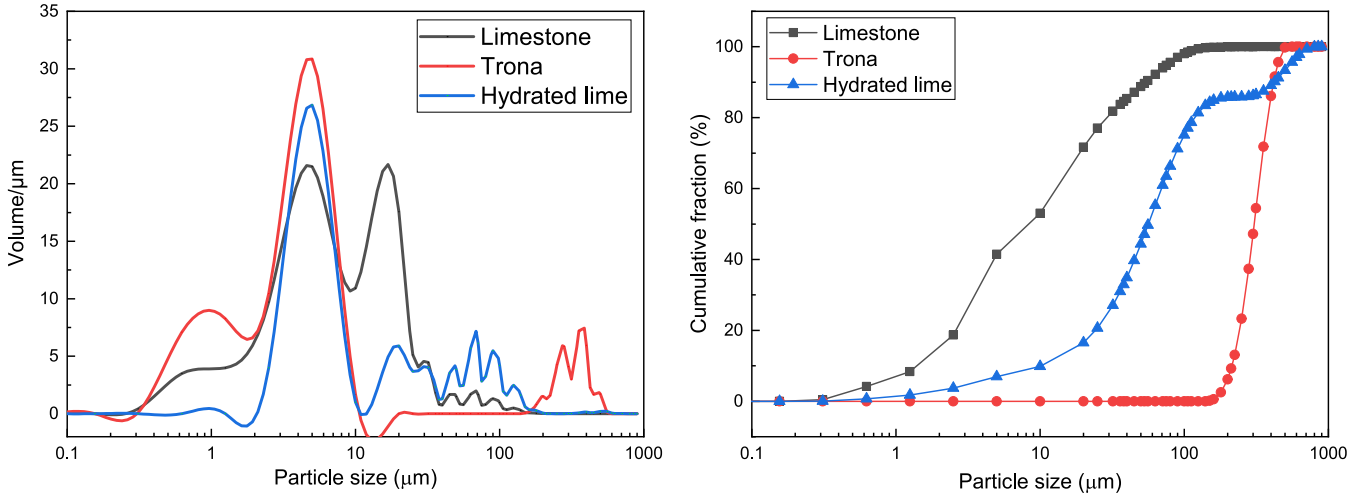

Figure 2. Particle size distribution of limestone, trona, and hydrated lime sorbents.

amount of 86.9 wt %. Trona, on the other hand, showed significant concentrations of Na_2O (51.58 wt %) based on XRF analysis, which indicated the presence of Na-bearing species such as $NaHCO_3$ (nahcolite). This was further confirmed by XRD analysis, which identified nahcolite in trona with a relative phase amount of 100.0 wt %. The contents of $CaCO_3$, $Ca[OH]_2$, and $NaHCO_3$ in the respective sorbents are crucial in terms of the total sulfation capacities of their slurries. The reactivities of these major components toward SO_2 also play an important role in the sulfation capacities[24] following the postulated reaction schemes presented in Appendix A. Particle size measurement of the sorbents (Figure 2) revealed that a significant proportion of the limestone sorbent had the finest particles ranging from 0 to 10 μm. Hydrated lime and trona had a greater fraction of coarse particles ranging from 10 to 1000 μm. Limestone and hydrated had the finest particles with a weighted mean value of 38.2 and 47.6 μm, respectively. Trona had significantly high weighted mean value of 130.8 μm also evidenced from the cumulative distribution of the sorbent particles.

3.2. Effects of Spray Drying Desulfurization Variables.

3.2.1. Stoichiometric Molar Ratio. The stoichiometric molar ratio in a spray drying scrubber system is defined as the mol flow ratio of fresh absorbent (Ca or Na) to SO_2 at the scrubber inlet. Figure 3 illustrates the effect of the stoichiometric molar ratio on SO_2 removal efficiency for hydrated lime, limestone, and trona. Generally, the results showed improved SO_2 removal efficiencies at high stoichiometric molar ratios for all sorbents, which is in agreement with observations made by others.[20,21,23] There was a steady monotonic increase in the removal efficiency when the stoichiometric molar ratio was increased. Trona had a high SO_2 removal efficiency (98%) at SR = 2.0 compared to hydrated lime (82%) at SR = 2.0 and limestone (59%) at SR = 1.75. The results also reveal that trona performed significantly better at a lower stoichiometric ratio (SR = 1.25) with a removal efficiency of 85%; hydrated lime and limestone had 45 and 41% SO_2 removal efficiency, respectively, at SR = 1.0. It is evident from Figure 3 that limestone has low reactivity toward SO_2 in the spray dryer over the range of experimental conditions, with a maximum value of 59% recorded at a stoichiometric molar ratio of 1.75. Hydrated lime had the largest increment of 49% in the removal efficiency when the stoichiometric molar ratio was varied from 1 to 2.5. It

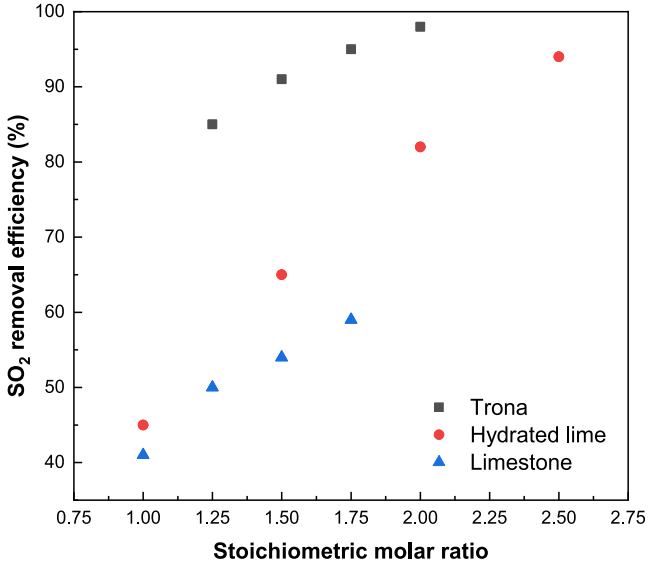

Figure 3. Effect of stoichiometric molar ratios on SO_2 removal efficiency for hydrated lime, limestone, and trona (slurry flow rate, 13 mL/min; inlet gas phase temperature, 140 °C; flue gas flow rate, 28 m^3/h; inlet SO_2 concentration, 1000 ppm).

has been reported that at a high stoichiometric molar ratio, there is increased sorbent particle concentration near the surface of the droplets, which reduces the liquid phase mass transfer resistance.[22,25] The increased sorbent particles provide sufficient Ca^{2+} ions at the droplet interface area, thereby accelerating the neutralization reaction with the dissociated ionic sulfur species at the reaction front.

3.2.2. Inlet Gas Phase Temperature. Figure 4 shows the influence of inlet gas phase temperature on SO_2 removal efficiency for the three sorbents. In all cases, there was a steady decline in the removal efficiency with increasing temperature. The experimental results show that trona had the highest removal efficiency (up to 90% at 120°C) compared with hydrated lime (82%) and limestone (76%). Limestone had the lowest SO_2 removal efficiency with a significant reduction of 34% between 120 and 180°C. Trona and hydrated lime showed SO_2 removal reduction of 9 and 6% drop, respectively, in the same temperature range. High temperature in a spray drying system lowers the solubility of SO_2 and $Ca[OH]_2$ in the

https://doi.org/10.1021/acsomega.3c00064
ACS Omega 2023, 8, 23401−23411

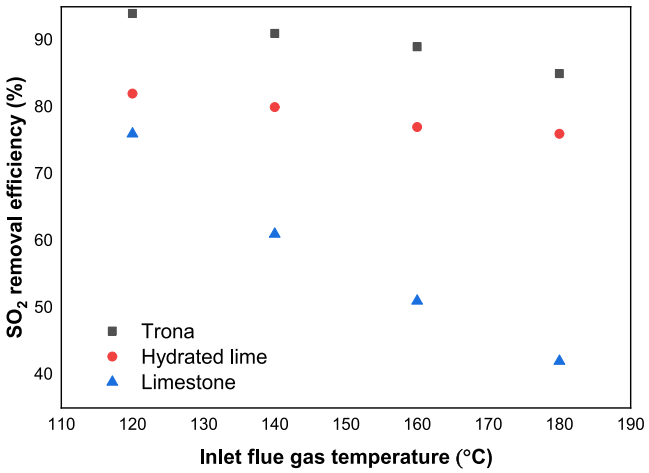

Figure 4. Effect of inlet gas phase temperature on SO_2 removal efficiency (SR, 1.5; slurry flow rate, 13 mL/min; flue gas flow rate, 28 m^3/h; inlet SO_2 concentration, 1000 ppm).

liquid phase and reduces the relative humidity resulting in an increased evaporation rate and subsequent depletion of water liquid volume for SO_2 absorption.[26,27] According to the associated chemical reactions (Appendix A), SO_2 initially dissolves and ionizes before reacting with the sorbent species. High temperatures accelerate the droplet evaporation rate in the spray dryer, significantly reducing the period required for SO_2 absorption.

3.2.3. Sorbent Performance and Mechanisms. The desulfurization process within a spray dryer using the three sorbents involves a complex and intricate series of subprocesses, as depicted in Appendix A. These processes comprise multiphase interplays and ionic reactions involving (a) gas–solid reaction between the adsorbed SO_2 and the solid sorbent and (b) liquid phase reaction between the dissolved sulfur species and the dissociated alkaline sorbent species.[38] According to Hill and Zank,[22] a number of factors are considered rate-controlling within the spray drying system. In the liquid phase, the dissolution of the solid phase plays a vital role in controlling the rate, with the mass transfer rate being influenced by several factors such as solid properties (solubility, particle size, and shape) and liquid characteristics such as pH and composition.[2] As the droplet starts to dry, it forms a solid crust composed of reaction products on its surface, and the diffusion through the reaction product layer becomes the new rate-controlling step.[39]

In comparison with limestone and hydrated lime, trona has a high chemical affinity to water, making it readily soluble in water, forming Na^+ ions in solution.[28] It dissolves completely in water to form a clear solution with no suspended undissolved particles. This property eliminates the effect of sorbent dissolution resistance within the droplet in the spray dryer, thus allowing rapid reaction between the dissociated sulfur and alkaline (Na^+ ions) species at the droplet interface (see Appendix A for the associated chemical reactions). On the other hand, hydrated lime and limestone are slightly soluble in water, prompting the additional resistance stemming from particle dissolution. This effect contributes to lower SO_2 absorption efficiencies in comparison with trona, as observed in the experimental findings. The variation in the performance of hydrated and limestone is attributed to the difference in their solubilities in water and reactivity toward SO_2. The solubility of $Ca[OH]_2$ in water at 20 °C is 0.165%, while $CaCO_3$ is 0.00066% at the same temperature.[29] The slow dissolution of limestone negatively impacts the rate of dissociation of Ca^{2+} ions into the solution, which is necessary for the neutralization reaction with the dissociated sulfur species (as shown in Appendix A). Furthermore, it is recognized that high alkalinity increases both the dissociation of SO_2 species and the rate of the neutralization reaction in the liquid phase.[30,31] Limestone dissolves in water to form a slurry with a pH ranging from 8 to 9, while hydrated lime slurries have a pH of around 12.[29] Due to the difference in the pH of their slurries, hydrated lime slurries have higher neutralizing rates than limestone slurries. This effect is evident from the experimental results, where hydrated lime performed better than limestone in the absorption of SO_2 for all of the experiments conducted.

The performance of the sorbents, especially for the slightly soluble sorbents (hydrated lime and limestone) in spray drying is partially dependent on the particle size ascribed to the volume-to-surface area ratio. Sorbents with finer particles are expected to perform better on account of the neutralization reaction which occurs at the surface of the unreacted sorbent particle.[32] On the contrary, hydrated lime performed better than limestone under all of the experimental conditions. This is attributable to factors such as higher solubility in water and the neutralizing capacity of hydrated lime against limestone as explained before. The extent of SO_2 removal observed is affected not only by chemical reactions but also by mass transfer, which is in turn influenced by fluid dynamics in the absorber.

3.3. Sorbent Utilization and Conversion. Table 4 presents the results of chemical analysis (XRD analysis) of the dried products, at different stoichiometric molar ratios, for all three sorbents studied. A general trend observed was the increasing concentration of unreacted sorbent ($Ca[OH]_2$, $CaCO_3$, and $NaHCO_3$) with increasing stoichiometric molar ratios. The final product collected from trona had significant concentrations of 44.4 wt % $NaHCO_3$ at SR = 2.0 compared to 34.7 wt % $NaHCO_3$ concentration at SR = 1.0. Although trona sorbent exhibited low sorbent utilization at a high stoichiometric ratio of 2.0, it achieved a high SO_2 removal efficiency of

Table 4. Desulfurization Product Compositions (wt %) at Various Stoichiometric Molar Ratios (SR), Determined from XRD Analyses

	initial sorbent sample	SR = 1.0	SR = 1.5	SR = 2.0
hydrated lime				
$Ca[OH]_2$	86.9	53.4	57.6	60.2
$CaSO_3$	0.0	43.6	40.2	38.1
$Mg[OH]_2$	1.1	0.4	0.5	0.5
$MgSO_3$	0.0	0,6	0.6	0.6
limestone				
$CaCO_3$	95.3	73.3	74.5	77.5
$CaSO_3$	0.0	21.7	24.6	21.7
$Mg[OH]_2$	2.0	1.5	1.5	1.6
$MgSO_3$		0.4	0.4	0.3
trona				
$Na_2CO_3/NaHCO_3$	100.0	34.7	35.6	44.4
Na_2SO_3	0.0	63.3	62.7	53.8
Na_2SO_4	0.0	1.0	0.8	0.8

https://doi.org/10.1021/acsomega.3c00064
ACS Omega 2023, 8, 23401−23411

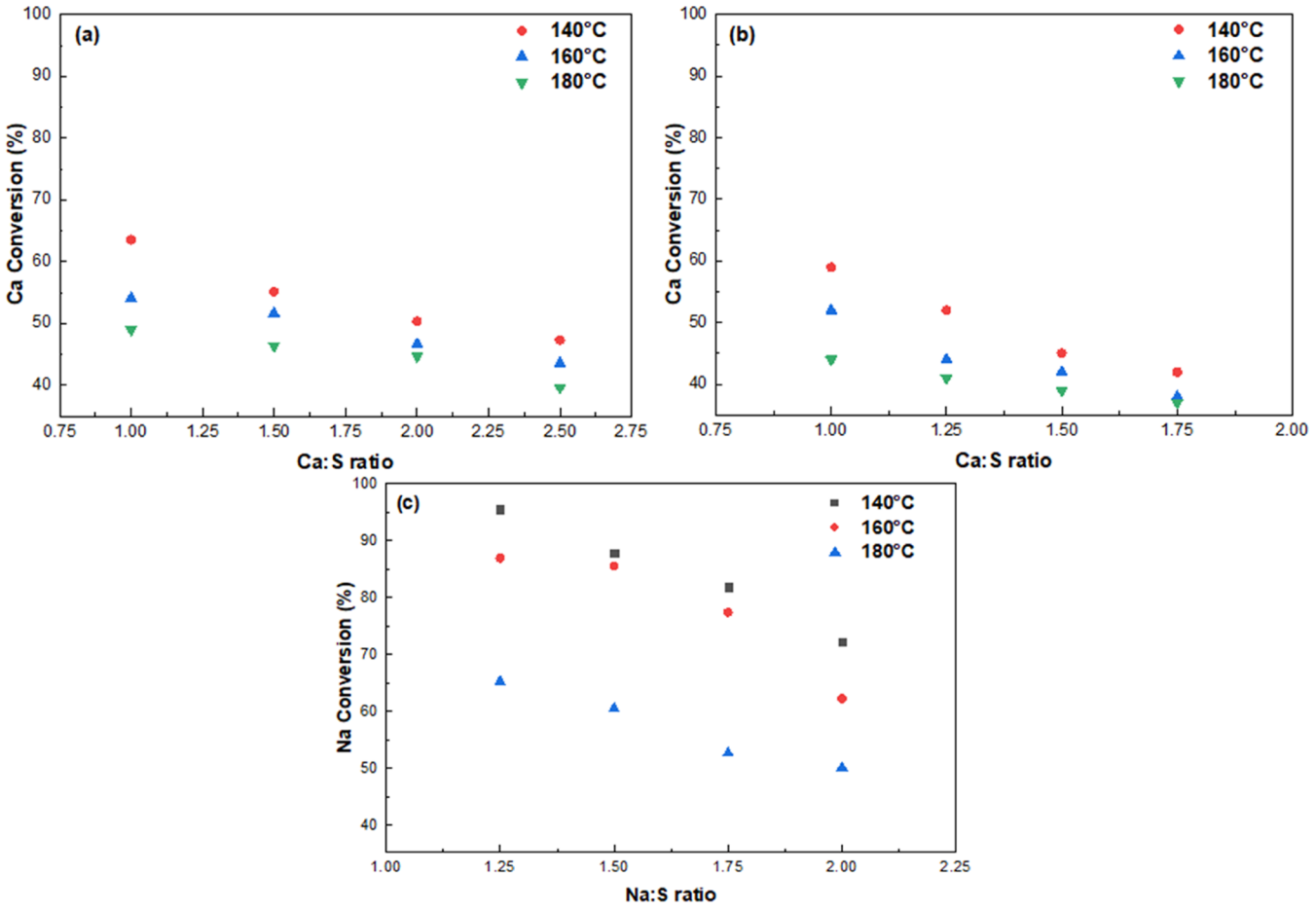

Figure 5. Degree of conversion at different stoichiometric molar ratios for (a) hydrated lime, (b) limestone, and (c) trona.

98%. Experimental results in Table 4 also indicate that the desulfurization products obtained at a stoichiometric molar ratio of 1.0 for hydrated lime and limestone contain slightly lower concentrations of unreacted $Ca[OH]_2$ (53.4 wt %) and $CaCO_3$ (73.3 wt %), respectively, compared to products obtained at SR = 2.0. This comparison demonstrates better sorbent conversion at lower stoichiometric ratios for both hydrated lime and limestone.

A theoretical assessment of the conversion of the sorbent was carried out based on the degree of conversion of the sorbent after SO_2 absorption. The degree of sorbent conversion x_{SB} was determined using eq 1

$$x_{SB} = \frac{n_{SO_{2,i}} - n_{SO_{2,o}}}{n_{SB_i}} \quad (1)$$

where:

SB is the sorbent (either Na for trona or Ca for hydrated lime and limestone),

n_{SB_i} is the molar flow rate of the sorbent in the feed slurry (mol/h),

$n_{SO_{2,i}}$ is the molar flow rate of the SO_2 in the flue gas inlet (mol/h), and

$n_{SO_{2,o}}$ is the molar flow rate of the SO_2 in the flue gas outlet (mol/h).

Figure 5 presents the degree of conversion of hydrated lime, trona, and limestone under various inlet gas phase temperatures (140−180 °C) and stoichiometric molar ratios (1.0−2.5). Generally, there was a high conversion for all sorbents at low temperatures, as observed at 140 °C. Besides the better absorption efficiency of trona toward SO_2, it exhibited the highest conversion, up to 96% at 140 °C, at a Ca:S ratio of 1.0. However, there was a significant drop in its conversion at the higher temperatures of 160 and 180°C. Hydrated lime and limestone achieved maximum conversions of 66 and 59%, respectively, at 140 °C. The chemical analysis of the dried product for hydrated lime and limestone shows evidence of low sorbent conversion (Table 4). Recirculation of a significant amount of the spent sorbent will therefore be required to improve its utilization. Low conversion for all of the sorbents at high temperatures (180 °C) was observed mainly due to an accelerated droplet evaporation rate, which limits the droplet's lifetime for SO_2 absorption and sorbent conversion. These observations are in good agreement with the literature and have been attributed to negligible internal mass transfer resistances for SO_2 at high stoichiometric ratios.[33] The prime objective of a scrubbing system is to remove SO_2 from flue gases to ranges within the applicable regulatory limits. South African regulatory requirement on SO_2 emission for large-scale coal utility plants is 1000 mg/Nm^3 (382 ppm).[34] Based on the setup used in this study, trona exhibited better performance characteristics toward the absorption of SO_2, with the exiting treated flue gas containing less than 100 ppm at stoichiometric molar ratios above 1.5.

3.4. Analysis of the Final Product of Desulfurization.

3.4.1. SEM Analysis. SEM analysis was carried out to observe qualitative changes in the chemical and crystal structures of the

https://doi.org/10.1021/acsomega.3c00064
ACS Omega 2023, 8, 23401−23411

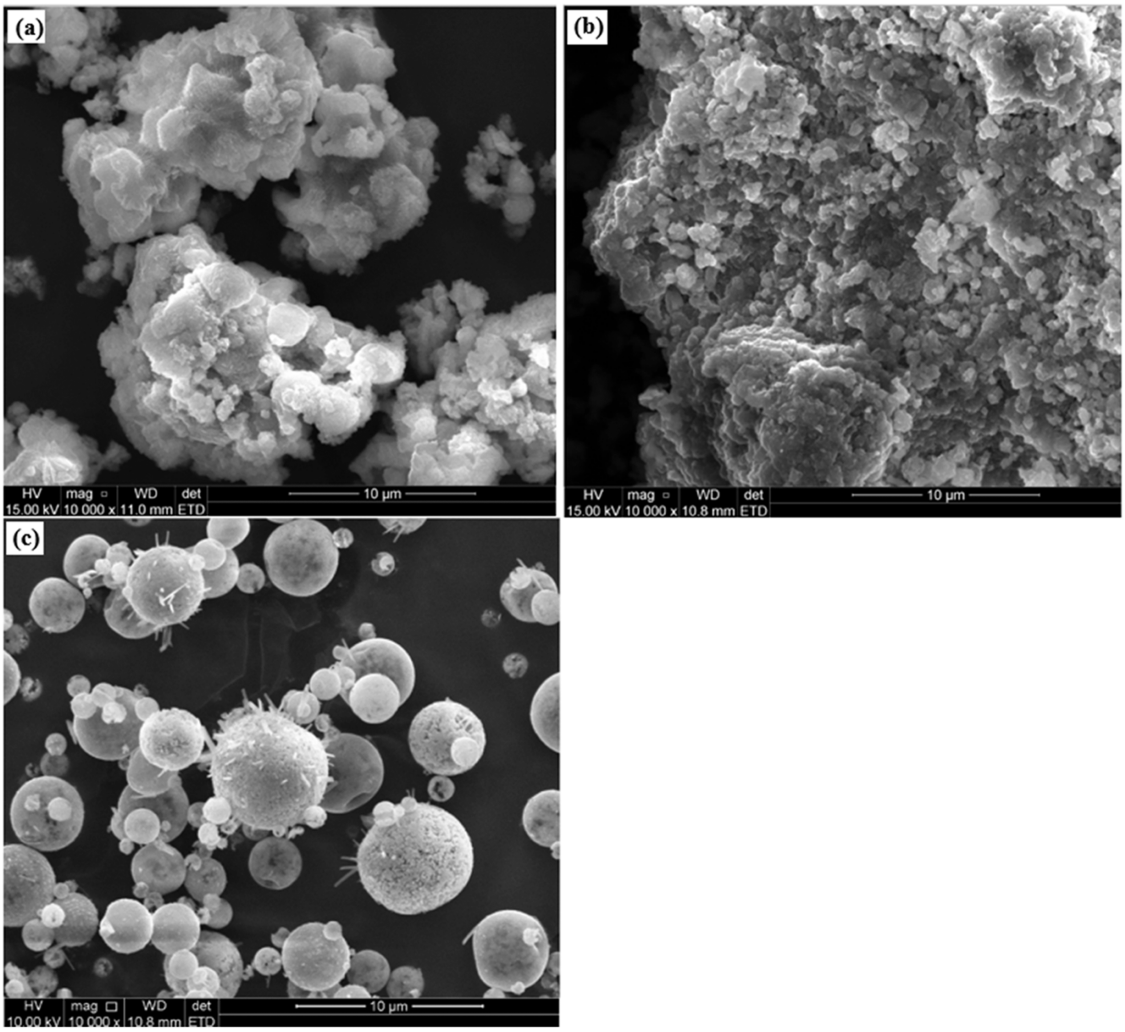

Figure 6. SEM micrographs of desulfurization products for (a) hydrated lime, (b) limestone, and (c) trona (SR = 1.5, inlet gas phase temperature = 140 °C).

sorbent samples during desulfurization. Figure 6a–c shows SEM micrographs of desulfurization product samples for hydrated lime, limestone, and trona sorbents. The samples were collected under the same experimental conditions: inlet gas phase temperature of 140 °C and SR = 1.5. Figure 6a shows a SEM micrograph for a hydrated lime desulfurization product, showing particles with rough surfaces agglomerated together, and partially reacted particles aggregating to form larger particles. Figure 6b shows a SEM micrograph for a limestone desulfurization product, revealing more aggregated particles; these would potentially limit exposure of unreacted particles and result in poor sorbent utilization, as is confirmed by XRD analysis (Table 4). Figure 6c shows a SEM micrograph for a trona desulfurization product, revealing spherical particles with mostly smooth surfaces. The effect of desulfurization on trona is evident from the relative roughness observed on some particles and the needle-like crystals on the particle surfaces, attributable to sulfite formation.

3.4.2. FTIR Analysis. The functional groups on the surface of the desulfurization product samples were determined by FTIR analysis (spectral range 350–4500 cm^{-1}). Figure 7 shows FTIR spectra for the desulfurization products of hydrated lime, limestone, and trona sorbents. The FTIR spectrum of the limestone desulfurization product shows strong absorption bands at 2520, 1402, 874, and 712 cm^{-1}, representing the presence of unreacted $CaCO_3$ (calcite) in the sample.[35] This observation confirms poor sorbent conversion, as also observed in XRD analysis (Table 4), and the degree of conversion (Figure 5). The FTIR spectrum of the hydrated lime desulfurization product shows absorption bands at 712, 875, and 1413 cm^{-1}, representing unreacted $Ca[OH]_2$ (portlandite) in the sample. The spectra for hydrated lime and limestone desulfurization products also show absorption bands at 652, 938, and 988 cm^{-1}, attributable to $CaSO_3{\cdot}0.5H_2O$.[36,37] This observation corresponds with the findings of XRD analysis, indicating the presence of sulfite in the samples. The relatively strong absorption peaks of $CaSO_3{\cdot}0.5H_2O$ in the hydrated lime desulfurization product, particularly at 652 and 938 cm^{-1}, is evidence of better sorbent conversion compared to the case of limestone. The FTIR spectrum of the trona desulfurization product shows strong absorption bands of sulfite ions, appearing around 1000–940 cm^{-1} and 650–520 cm^{-1}. These are products of the absorption reaction between the sorbent and SO_2, resulting in the formation of SO_3^{2-} in the final product. The absorption bands appearing around 1726 and 1432 cm^{-1} represent unreacted Na_2CO_3 in the desulfurization product.

https://doi.org/10.1021/acsomega.3c00064
ACS Omega 2023, 8, 23401–23411

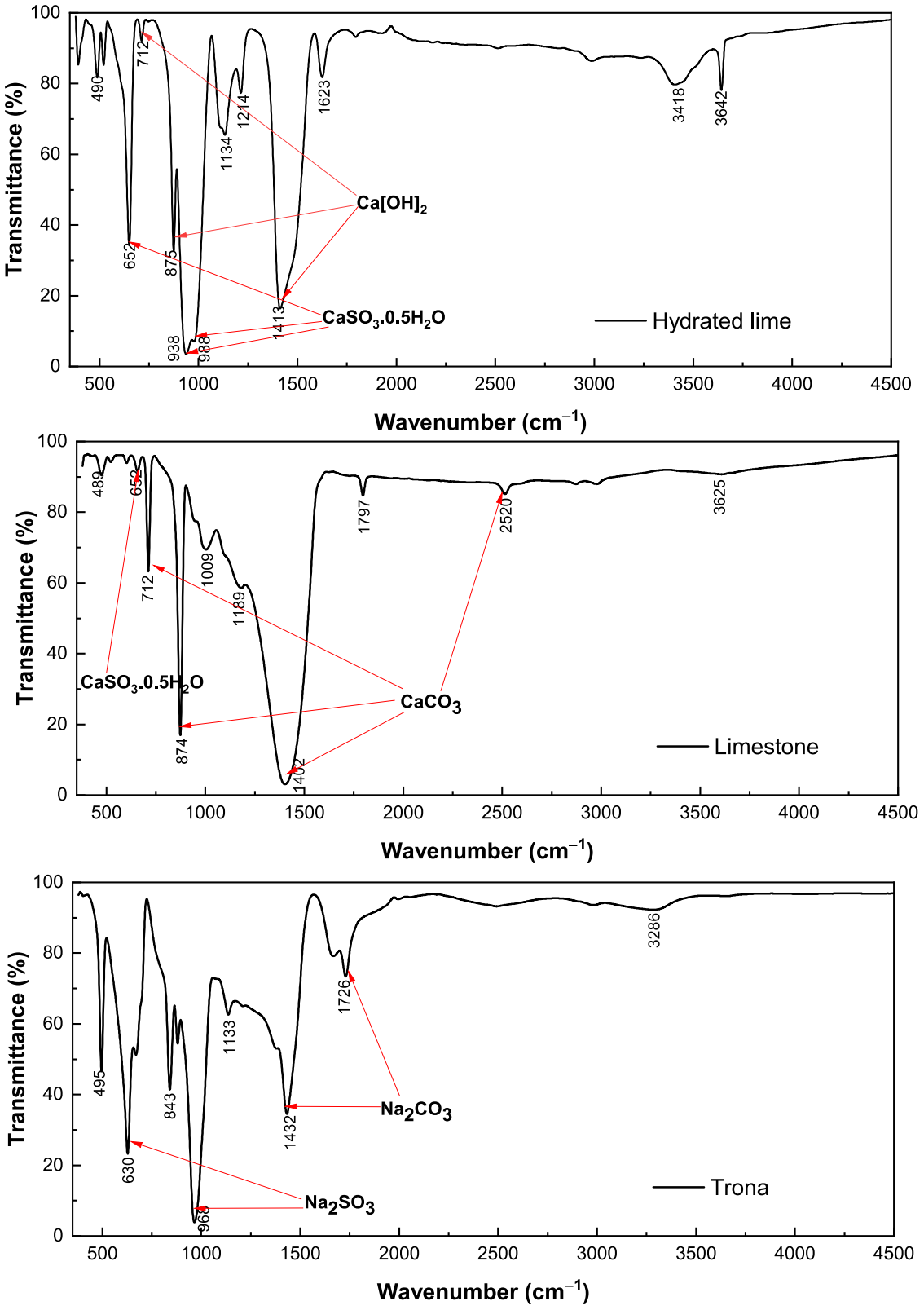

Figure 7. FTIR spectra of desulfurization products, for hydrated lime, limestone, and trona sorbents.

4. CONCLUSIONS

Desulfurization experiments were carried out with sorbents (hydrated lime, limestone, and trona), using a laboratory-scale spray dryer, and their performance characteristics for the absorption of SO_2 were compared. Trona and hydrated lime exhibited the highest SO_2 removal efficiency of 98 and 82%, respectively, at a stoichiometric ratio of 2.0; the SO_2 removal efficiency of limestone was 59% at a stoichiometric molar ratio of 1.75. Although all sorbents feature a decline in SO_2 removal with increasing inlet gas phase temperatures, limestone had the largest drop in the removal efficiency, from 76 to 42% between

https://doi.org/10.1021/acsomega.3c00064
ACS Omega 2023, 8, 23401−23411

120 and 180 °C. Trona slurry had rapid neutralization of the sulfur species due to low mass transfer resistance arising from high chemical affinity to water. Hydrated lime slurry performed better than limestone due to higher solubility and neutralizing rates than limestone. XRD and FTIR analyses of the desulfurization products indicated significant conversion of the trona sorbent compared to hydrated lime and limestone. High concentrations of the unreacted sorbent, at a stoichiometric molar ratio of 2, for hydrated lime (60%) and limestone (77%) were observed in their respective final product samples, in comparison with trona (44%). Overall, a comparison of the spray dryer performance, based on SO_2 removal efficiency, sorbent utilization, and analysis of the desulfurization products, revealed that trona gave better performance characteristics in the spray dyer setup used compared to hydrated lime and limestone sorbents.

Further research to develop a better understanding of the spray dry scrubbing performance with the different sorbents is recommended. It is proposed that investigations be undertaken confined to the assessment and analyses of the flow dynamics (residence times), the interfacial heat and mass transfer, and the associated chemical reactions. For this purpose, advanced computational fluid dynamics modeling can be used. It is also recommended that the droplet particle size be considered as an important parameter in spray dry scrubbing process.

APPENDIX A: ASSOCIATED CHEMICAL REACTIONS

Spray dry scrubbing of SO_2 is a process involving sorbent dissolution and SO_2 gas absorption into the alkaline slurry droplet with a series of reactions in the liquid phase within the spray dryer. The following scheme of reactions is postulated to occur in the spray dry scrubbing of SO_2 using hydrated lime, limestone, and trona:[16,22,32]

Dissolution of the sorbent into respective alkaline species in the liquid phase

- Limestone

$$CaCO_{3(s)} + H_2O_{(l)} \rightarrow Ca^{2+}_{(aq)} + CO^{2-}_{3(aq)} + H_2O_{(l)} \quad (2)$$

- Hydrated lime

$$Ca[OH]_{2(s)} + H_2O_{(l)} \rightarrow Ca^{2+}_{(aq)} + 2OH^{-}_{(aq)} + H_2O_{(l)} \quad (3)$$

- Trona

$$Na_2CO_3{\cdot}NaHCO_3{\cdot}2H_2O_{(s)} + H_2O_{(l)} \rightarrow 3Na^{+}_{(aq)} + 2CO^{-}_{3(aq)} + 3OH^{-}_{(aq)} + 6H^{+}_{(aq)} \quad (4)$$

The dissolved SO_2 reacts with water to form sulfurous acid and dissociates into ionic sulfur species.

$$SO_{2(aq)} + H_2O_{(l)} \rightarrow H_2SO_{3(aq)} \quad (5)$$

$$H_2SO_{3(aq)} \leftrightarrow H^{+}_{(aq)} + HSO^{-}_{3(aq)} \quad (6)$$

$$HSO^{-}_{3(aq)} \leftrightarrow H^{+}_{(aq)} + SO^{2-}_{3(aq)} \quad (7)$$

Neutralization reaction between the dissolved alkaline and acid species at the reaction front to form sulfite product.

- Hydrated lime and limestone

$$Ca^{2+}_{(aq)} + SO^{2-}_{3(aq)} + 0.5H_2O_{(l)} \rightarrow CaSO_3{\cdot}0.5H_2O_{(s)} \quad (8)$$

- Trona

$$2Na^{+}_{(aq)} + 2OH^{-}_{(aq)} + SO^{2-}_{3(aq)} + H_2O_{(l)} \rightarrow Na_2SO_{3(s)} + 2H_2O_{(l)} \quad (9)$$

The overall reactions between SO_2 and the respective sorbents are expressed as follows:

- Hydrated lime

$$Ca(OH)_{2(s)} + SO_{2(g)} + 0.5H_2O_{(l)} \rightarrow CaSO_3{\cdot}0.5H_2O_{(s)} + H_2O_{(l)} \quad (10)$$

- Hydrated lime

$$CaCO_{3(s)} + SO_{2(g)} + 0.5H_2O_{(l)} \rightarrow CaSO_3{\cdot}0.5H_2O_{(s)} + CO_{2(g)} \quad (11)$$

- Trona

$$2Na_2CO_3{\cdot}NaHCO_3{\cdot}2H_2O_{(s)} + 3SO_{2(g)} + H_2O_{(l)} \rightarrow 3Na_2SO_{3(s)} + 6H_2O_{(l)} + 4CO_{2(g)} \quad (12)$$

AUTHOR INFORMATION

Corresponding Author

Lawrence Koech − *Eskom Power Plant Engineering Institute (EPPEI) Specialization Centre for Emission Control, School of Chemical and Minerals Engineering, Centre of Excellence in Carbon-based Fuels, North-West University, Potchefstroom 2520, South Africa; Department of Chemical and Metallurgical Engineering, Vaal University of Technology, Vanderbijlpark 1900, South Africa;* orcid.org/0000-0003-1179-9594; Phone: +27 (0) 16 9504762; Email: lawrencek@vut.ac.za

Authors

Raymond C. Everson − *Eskom Power Plant Engineering Institute (EPPEI) Specialization Centre for Emission Control, School of Chemical and Minerals Engineering, Centre of Excellence in Carbon-based Fuels, North-West University, Potchefstroom 2520, South Africa*

Burgert Hattingh − *Eskom Power Plant Engineering Institute (EPPEI) Specialization Centre for Emission Control, School of Chemical and Minerals Engineering, Centre of Excellence in Carbon-based Fuels, North-West University, Potchefstroom 2520, South Africa*

Hilary Rutto − *Eskom Power Plant Engineering Institute (EPPEI) Specialization Centre for Emission Control, School of Chemical and Minerals Engineering, Centre of Excellence in Carbon-based Fuels, North-West University, Potchefstroom 2520, South Africa; Department of Chemical and Metallurgical Engineering, Vaal University of Technology, Vanderbijlpark 1900, South Africa*

Letsabisa Lerotholi − *Eskom Power Plant Engineering Institute (EPPEI) Specialization Centre for Emission Control, School of Chemical and Minerals Engineering, Centre of Excellence in Carbon-based Fuels, North-West University, Potchefstroom 2520, South Africa; Department of Chemical*

https://doi.org/10.1021/acsomega.3c00064
ACS Omega 2023, 8, 23401−23411

and Metallurgical Engineering, Vaal University of Technology, Vanderbijlpark 1900, South Africa

Hein WJP Neomagus − *Eskom Power Plant Engineering Institute (EPPEI) Specialization Centre for Emission Control, School of Chemical and Minerals Engineering, Centre of Excellence in Carbon-based Fuels, North-West University, Potchefstroom 2520, South Africa*

Complete contact information is available at: https://pubs.acs.org/10.1021/acsomega.3c00064

Notes

The authors declare no competing financial interest.

■ ACKNOWLEDGMENTS

The authors acknowledge the financial support received from the Eskom Power Plant Engineering Institute (EPPEI), particularly for the financial support provided to Lawrence Koech as a student at the EPPEI Emissions Control Specialisation Centre and the Vaal University of Technology.

■ REFERENCES

(1) Kumar, L.; Jana, S. K. Advances in absorbents and techniques used in wet and dry FGD: a critical review. *Rev. Chem. Eng.* **2022**, *38*, 843−880.

(2) Koech, L.; Rutto, H.; Lerotholi, L.; Everson, R. C.; Neomagus, H.; Branken, D.; Moganelwa, A. Spray drying absorption for desulphurization: a review of recent developments. *Clean Technol. Environ. Policy* **2021**, *23*, 1665−1686.

(3) Liu, F.; Cai, M.; Liu, X.; Zhu, T.; Zou, Y. O_3 oxidation combined with semi-dry method for simultaneous desulfurization and denitrification of sintering/pelletizing flue gas. *J. Environ. Sci.* **2021**, *104*, 253−263.

(4) Yu, Y. P.; Fang, Y.; Chai, S. Y.; Zhuang, Z. Z. In *Properties of Semi-Dry Flue Gas Desulfurization Ash and Used for Phosphorus Removal*, IOP Conference Series: Materials Science and Engineering, November 17-19; IOP Publishing: Yichang, China, 2017012021 DOI: 10.1088/1757-899X/359/1/012021.

(5) Rogoff, M. J.; Screve, F. Permitting Issues. In *Waste-to-Energy: Technologies and Project Implementation*, 3rd ed.; Rogoff, M. J.; Screve, F., Eds.; William Andrew Publishing, 2019; pp 117−148.

(6) GEA. GEA Niro spray drying absorption: The easy way to clean the flue gas from waste incinerators *GEA Process Engineering* 2022 https://www.gea.com/en/products/emission-control/sorption/spray-dryer-absorber.jsp (accessed October 20, 2022).

(7) Poullikkas, A. Review of Design, Operating, and financial considerations in flue gas desulfurization systems. *Energy Technol. Policy* **2015**, *2*, 92−103.

(8) Sharifi, N. P.; Jewell, R. B.; Duvallet, T.; Oberlink, A.; Robl, T.; Mahboub, K. C.; Ladwig, K. J. The utilization of sulfite-rich Spray Dryer Absorber Material in portland cement concrete. *Constr. Build. Mater.* **2019**, *213*, 306−312.

(9) EPRI (Electric Power Research Institute). *CoalFleet Guideline for Advanced Pulverized Coal Power Plants*, 1019674; 2010 222 Advanced Generation & Carbon Capture and Storage, 2010 https://www.epri.com/research/products/1019674 (accessed August 14, 2022).

(10) Carpenter, A. M. *Low water FGD technologies CCC/210*; IEA Clean Coal Centre: London, 2012.

(11) França, Í. W.; Cartaxo, S. J.; Bastos-Neto, M.; Gonçalves, L. R.; Fernandes, F. A. Effect of Additives to Improve Calcium-Based Sorbents in Semi-Dry Flue Gas Desulphurization. *Emiss. Control Sci. Technol.* **2020**, *6*, 105−112.

(12) Srivastava, R. K. *Controlling SO2 Emissions--A Review of Technologies*, EPA/600/R-00/093; U.S. Environmental Protection Agency, Office of Research and Development: Washington, D.C., 2000 https://cfpub.epa.gov/si/si_public_record_report.cfm?Lab=NRMRL&dirEntryId=18978 (accessed April 15, 2022).

(13) Fischer, M.; Darling, G. Circulating fluidized bed scrubber vs spray dryer absorber. Power Engineering. September 14, 2015, https://www.power-eng.com/emissions/policy-regulations/circulating-fluidized-bed-scrubber-vs-spray-dryer-absorber/ (accessed January 12, 2022).

(14) Yang, H. M.; Kim, S. S. Experimental study on the spray characteristics in the spray drying absorber. *Environ. Sci. Technol.* **2000**, *34*, 4582−4586.

(15) Tang, W.; Zhang, L.; Luo, H. Experimental Study on the Removal of Low-Concentration SO3 by Trona at Medium Temperatures. *Ind. Eng. Chem. Res.* **2021**, *60*, 8947−8956.

(16) Erdöl-Aydın, N.; Nasün-Saygılı, G. Modelling of trona based spray dry scrubbing of SO2. *Chem. Eng. J.* **2007**, *126*, 45−50.

(17) Tomás-Alonso, F. A new perspective about recovering SO2 offgas in coal power plants: energy saving. Part II. Regenerable dry methods. *Energy Sources* **2005**, *27*, 1043−1049.

(18) Maziuk, J. Dry sorbent injection of trona for SOx mitigation. In 67th conference on glass problems. *Ceram. Eng. Sci. Proc.* **2009**, *28*, 85−99.

(19) Buchi. B-290 Mini Spray Dryer Operation Manual, 2018 https://www.buchi.com/en/products/instruments/mini-spray-dryer-b-290 (accessed April 12, 2022).

(20) Xie, D.; Wang, H.; Chang, D.; You, C. Semidry desulfurization process with in-situ supported sorbent preparation. *Energy Fuels* **2017**, *31*, 4211−4218.

(21) Scala, F.; Lancia, A.; Nigro, R.; Volpicelli, G. Spray-dry desulfurization of flue gas from heavy oil combustion. *J. Air Waste Manage. Assoc.* **2005**, *55*, 20−29.

(22) Hill, F. F.; Zank, J. Flue gas desulphurization by spray dry absorption. *Chem. Eng. Process.: Process Intensif.* **2000**, *39*, 45−52.

(23) Doğu, G.; Uçar, Ç.; Doğu, T.; Gürüz, G.; Durmaz, A.; Ercan, Y. Scrubbing of SO2 with trona solution in a spray drier. *Can. J. Chem. Eng.* **1992**, *70*, 808−813.

(24) Gutiérrez Ortiz, F. J.; Vidal, F.; Ollero, P.; Salvador, L.; Cortés, V.; Gimenez, A. Pilot-plant technical assessment of wet flue gas desulfurization using limestone. *Ind. Eng. Chem. Res.* **2006**, *45*, 1466−1477.

(25) Gao, H.; Li, C.; Zeng, G.; Zhang, W.; Shi, L.; Li, S.; Zeng, Y.; Fan, X.; Wen, Q.; Shu, X. Flue gas desulphurization based on limestone-gypsum with a novel wet-type PCF device. *Sep. Purif. Technol.* **2011**, *76*, 253−260.

(26) Córdoba, P. Status of Flue Gas Desulphurisation (FGD) systems from coal-fired power plants: Overview of the physic-chemical control processes of wet limestone FGDs. *Fuel* **2015**, *144*, 274−286.

(27) Fakhari, M. A.; Rahimi, A.; Hatamipour, M. S.; Fozooni, A. Experimental study of simultaneous removal of CO2 and SO2 in a spouted bed reactor. *Can. J. Chem. Eng.* **2017**, *95*, 1150−1155.

(28) Kim, J.; Lee, J. Y.; Lu, T. Enhanced autotrophic growth of Nannochloris sp. with trona buffer for sustainable carbon recycle. *Biotechnol. Bioprocess Eng.* **2016**, *21*, 422−429.

(29) Haynes, W. M. *Handbook of Chemistry and Physics*, 97th ed.; CRC Press, 2016.

(30) Grinišin, N.; Bešenić, T.; Kozarac, D.; Živić, M.; Wang, J.; Vujanović, M. Modelling of absorption process by seawater droplets for flue gas desulfurization application. *Appl. Therm. Eng.* **2022**, *215*, No. 118915.

(31) Wang, B.; Yang, G.; Tian, H.; Li, X.; Yang, G.; Shi, Y.; Zhou, Z.; Zhang, F.; Zhang, Z. A new model of bubble Sauter mean diameter in fine bubble-dominated columns. *Chem. Eng. J.* **2020**, *393*, No. 124673.

(32) Ma, X.; Kaneko, T.; Tashimo, T.; Yoshida, T.; Kato, K. Use of limestone for SO2 removal from flue gas in the semidry FGD process with a powder-particle spouted bed. *Chem. Eng. Sci.* **2000**, *55*, 4643−4652.

(33) Katolicky, J.; Jicha, M. Influence of the Lime Slurry Droplet Spectrum on the Efficiency of Semi-Dry Flue Gas Desulfurization. *Chem. Eng. Technol.* **2013**, *36*, 156−166.

(34) Department of Home Affairs, South Africa. Amendment of the Listed Activities and Associated Minimum Emission Standards:

National Environmental Management: Air Quality Act, 2004 (Act No. 39 of 2004) 2020 https://www.dffe.gov.za/mediarelease/creecy_emmissionstandards_amendmentpromulgated_sulpurdioxide_combustioninstallation (accessed October 20, 2022).
(35) Hamed, M. M.; Ahmed, I. M.; Metwally, S. S. Adsorptive removal of methylene blue as organic pollutant by marble dust as eco-friendly sorbent. *J. Ind. Eng. Chem.* **2014**, *20*, 2370−2377.
(36) Navarrete, I.; Vargas, F.; Martinez, P.; Paul, A.; Lopez, M. Flue gas desulfurization (FGD) fly ash as a sustainable, safe alternative for cement-based materials. *J. Cleaner Prod.* **2021**, *283*, No. 124646.
(37) Pekov, I. V.; Chukanov, N. V.; Britvin, S. N.; Kabalov, Y. K.; Göttlicher, J.; Yapaskurt, V. O.; Zadov, A. E.; Krivovichev, S. V.; Schüller, W.; Ternes, B. The sulfite anion in ettringite-group minerals: a new mineral species hielscherite, Ca3Si(OH)6(SO4)(SO3).11H2O, and the thaumasite−hielscherite solid-solution series. *Mineral. Mag.* **2012**, *76*, 1133−1152.
(38) Irabien, A.; Cortabitarte, F.; Ortiz, M. I. Kinetics of Flue Gas Desulfurization at Low Temperatures: Nonideal Surface Adsorption Model. *Chem. Eng. Sci.* **1992**, *47*, 1533−1543.
(39) Karlsson, H. T.; Klingspor, J. Tentative Modelling of Spray-dry Scrubbing of SO2. *Chem. Eng. Technol.* **1987**, *10*, 104−112.

https://doi.org/10.1021/acsomega.3c00064
ACS Omega 2023, 8, 23401−23411